Quantum CART (*qCART*), a *piggyBac*-based system for development and production of virus-free multiplex CAR-T cell therapy

Yi-Chun Chen[1], Wei-Kai Hua[1], Jeff C. Hsu[1], Peter S. Chang[1], Kuo-Lan Karen Wen[1], Yi-Wun Huang[1], Jui-Cheng Tsai[1], Yi-Hsin Kao[1], Pei-Hua Wu[1], Po-Nan Wang[2], Ke-Fan Chen[1], Wan-Ting Liao[1], Sareina Chiung-Yuan Wu[1,†]

[1]GenomeFrontier Therapeutics, Inc. Taipei City, Taiwan (R.O.C.)

[2]Division of Hematology, Chang Gung Medical Foundation, Linkou Branch, Taipei City, Taiwan (R.O.C.)

[†]To whom correspondence may be addressed. Sareina Chiung-Yuan Wu; 18F-1, No. 3, Park St., Nangang Dist., Taipei City 11503, Taiwan (R.O.C.); +886-2-26558766;

Email: sareina@genomefrontier.com

Author Contributions: S.C.-Y.W. designed research. Y.-C.C., W.-K.H., Y.-W.H., J.-C.T., Y.-H.K., P.-H.W., P.-N.W., K.-F.C., W.-T.L. performed research. J.C.H., Y.-C.C, W.-K.H., K.-L.K.W., and S.C.-Y.W. analyzed data. J.C.H., P.S.C. and S.C.-Y.W. wrote the paper.

Competing Interest Statement: S.C.-Y.W. is a founder of GenomeFrontier Therapeutics, Inc., Y.-C.C., W.-K.H., K.-L.K.W., Y.-W.H., J.-C.T., Y.-H.K., P.-H.W., K.-F.C., W.-T.L., P.S.C. and J.C.H. are affiliated with GenomeFrontier Therapeutics, Inc.

Classification: Biological Sciences, Medical Sciences.

Keywords: multiplex CAR-T | *piggyBac* | T_{SCM} | transposon

This PDF file includes:

Main Text
Figures 1 to 6
Tables 1 to 2

Abstract

Chimeric antigen receptor T (CAR-T) cell therapy has the potential to transform cancer treatment. However, CAR-T therapy application is currently limited to certain types of relapse and refractory liquid tumors. To unlock the full potential of CAR-T therapy, technologic breakthroughs will be needed in multiple areas, including optimization of autologous CAR-T development, shortening the innovation cycle, and further manufacturing advancement of next-generation CAR-T therapies. Here, we established a simple and robust virus-free multiplex *Quantum CART* (*qCART*™) system that seamlessly and synergistically integrates four platforms: 1. *GTailor*™ for rapid identification of lead CAR construct design, 2. *Quantum Nufect*™ for effective but gentle electroporation-based gene delivery, 3. *Quantum pBac*™, featuring a virus-free transposon-based vector with large payload capacity and potentially safe integration profile, and 4. *iCellar*™ for robust and high-quality CAR^+ T memory stem cell (T_{SCM}) expansion. This robust, virus-free multiplex *qCART*™ system is expected to unleash the full potential of CAR-T therapy for treating diseases.

Significance Statement

Chimeric antigen receptor T (CAR-T) cell therapy is currently ineffective against solid tumors. Here, we showcase *Quantum CART* (*qCART*™), a simple and robust system that seamlessly and synergistically integrates four platforms for optimal production of multiplex virus-free CAR-T cells: *GTailor*™ for rapid identification of lead CAR candidates; *Quantum Nufect*™ for effective but gentle electroporation-based gene delivery; *Quantum pBac*™, featuring a highly efficient, high payload capacity virus-free gene therapy vector and potentially safe integration profile; and *iCellar*™ for robust and high quality CAR-T cell expansion. We demonstrate that *qCART*™ is a simple and robust system for cost-effective and time-efficient manufacturing of T memory stem cell (T_{SCM}) multiplex CAR-T cells.

Main Text

Introduction

In recent decades, immunotherapy has revolutionized the field of oncology. T lymphocytes with the capacity for antigen-directed cytotoxicity and persistence, have taken center stage in the fight against cancer(1, 2). Among T cell-based therapies, chimeric antigen receptor T (CAR-T) therapies have the potential to transform cancer treatment(3–9). CAR combines the specificity of an antibody recognition domain with the cytolytic and stimulatory capabilities of T cells. In contrast to human leukocyte antigen (HLA) restriction requirement of natural T cells, CAR-T cells directly recognize and destroy target cells(10).

A successful CAR-T therapy requires not only tumor recognition, but also sufficient cell expansion, persistence, and delivery of effector function(s). Second generation CAR-T cells that incorporate CD28 or 4-1BB in the CAR design have demonstrated therapeutic efficacy against hematological malignancies(11–16). However, successful treatment against solid tumors remains a challenge due to the hostile immunosuppressive tumor microenvironment (TME) that inhibit the infiltration, survival, and cytotoxic activity of CAR-T lymphocytes (17–19). One strategy to overcome this challenge is to engineer CAR-T cells to express additional genes that enhance CAR-T functions, so called armored CAR-T cells(20). Efficacy of armored CAR-T therapies against solid tumors in preclinical studies has been well-documented, and clinical trials are currently ongoing(21–26). However, the repertoire of genes that can be included in armored CAR-T therapies are severely restricted by the limited cargo capacity of viral vectors. Another strategy for strengthening CAR-T efficacy is to enrich specific T cell subsets that possess superior capability to persist and attack cancer. Ever since Gattinoni *et al.* described a class of immunological memory cells known as memory stem T cell (T_{SCM})(27), several studies have demonstrated that T_{SCM} is critical in facilitating successful adoptive T cell therapy(28–31).

Currently, retroviral and lentiviral vectors are the most common vehicles used for CAR-T engineering(32, 33). However, virus-based CAR-T therapies have potential risk of genotoxicity and are unsuitable for multiplex CAR-T production due to limited gene cargo capacity. Furthermore, the high cost of virus-based CAR-T therapies prevents widespread patient accessibility. Until recently, non-virus-based CAR-T development has had limited success due to low gene transfer efficiency and difficulty to efficiently expand quality engineered T cells to clinical scale.

In this study, we describe the benefits of virus-free transposon-based genetic modification systems. We developed a robust system called *qCART*™, which addresses the shortcomings of conventional viral and virus-free CAR-T therapies. Furthermore, we demonstrate that *qCART*™ can generate multiplex CAR-T cells that express genes of interest with various targeting

specificities and sizes (>7.6 Kb). We show that the engineered CAR-T cells consistently exhibit desired features, including high T_{SCM} (>70%), high expansion capacity, and robust anti-tumor efficacy.

Given that *qCART*™ can shorten both the development and manufacturing timeline of virus-free multiplex CAR-T therapy (next-generation CAR-T therapy), *qCART*™ represents a technological breakthrough that will unlock the full potential of CAR-T therapies and promote widespread patient access.

Results

qCART™ system addresses unmet needs of conventional CAR-T therapies

To overcome current unmet needs of cancer gene therapy, we have developed a virus-free *Quantum Engine*™, a cell production system composed of four platforms: *GTailor*™, *Quantum Nufect*™, *Quantum pBac*™, and *iCellar*™. A schematic depiction of *qCART*™ (a *Quantum Engine*™ for CAR-T production) highlighting the roles of each platform is shown in Figure 1. The first platform, *GTailor*™, is a rapid multiplex gene design, construction, and screening system for designing CAR-T cells with (i) the ability to recognize multiple cancer targets; (ii) modulators for effective CAR-T trafficking, infiltration or TME resistance; and (iii) a safety control to terminate the treatment as needed. The second platform, *Quantum Nufect*™, is an electroporation-based gene delivery buffer system for introducing therapeutic genes into T cells while preserving high cell viability. The third platform, *Quantum pBac*™, is a virus-free transposon vector system with (i) a large payload capacity, (ii) highly efficient yet potentially safer genome integration, and (iii) high preference for T_{SCM} transposition(53). Finally, the fourth platform, *iCellar*™, is a cell expansion system for producing clinical-scaled CAR-T cells with (i) high percentage of CAR^+ T_{SCM} cells and (ii) enhanced fitness. As shown in the following sections, *qCART*™ overcomes major hurdles faced by current virus-based and virus-free gene delivery systems.

GTailor™ facilitates the design, construction, and screening of therapeutic gene constructs to identify lead candidates for preclinical development

Since identification of CAR-T lead candidates is laborious, time-consuming and requires multiple rounds of screening involving designing and construction of gene constructs and subsequent *in vitro* and/or *in vivo* testing and validation, we developed *GTailor*™ to streamline these processes for efficient lead candidate identification. The platform consists of the following technologies: (1) a library of functional modules for rapid establishment of a therapeutic construct bank, (2) a simple, time-effective and economical cell engineering process for building a multiplex

CAR-T cell library, (3) a high throughput *in vitro* cytotoxicity assay system for identifying CAR-T cells with the most potent, persistent, and safe profile, i.e. highest anti-tumor specific activity and lowest On-Target, Off-Tumor toxicity. An sample screening process for BCMA CAR-T cells is depicted in Supplementary Fig. S1, and the results are presented in Table 1. As shown, all five groups of CAR-T cells performed similarly and satisfactorily in terms of cell expansion (day 1 to 10 fold change), percentage of CAR^+ cells, CD8/CD4 ratio, and percentage of T_{SCM} in both CD4 and CD8 populations (Table 1). However, three CAR-T groups (aBCMA-1, aBCMA-3 and aBCMA-4) exhibited markedly lower cytotoxicity against $BCMA^+$ target cells. Note that the percentage of $PD1^+$ CAR-T cells in the aBCMA-3 group was also markedly higher than those found in other groups. CAR-T cells with undesired traits were tested at least twice (T cells derived from different donors), whereas those without these traits were tested at least three times to confirm reproducibility. As a result, only aBCMA-2 and aBCMA-5 CAR-T cells were identified as tentative candidates. Next, we assessed the efficacy and specificity of these two candidates by co-culturing each candidate CAR-T cells with a panel of BCMA-negative and BCMA-positive tumor and normal cells. As shown (Supplementary Table S5), aBCMA-5 lysed more cells expressing minimal/no BCMA, so we chose aBCMA-2 as the candidate for pipeline development.

Quantum pBac™ (_qPB_) facilitates consistent intra-cell type genome integration that are expected to be relatively safe

We previously demonstrated that the *qPB* system is superior compared to other *piggyBac* transposon systems(53). Since little is known regarding the integration characteristics of *qPB*, we analyzed for the first time, the integration profile of *qPB* in CAR-T cells. Additionally, we compared the *qPB* integration profile with that of human embryonic kidney (HEK293) cells (34) to determine whether there may be any inter-cell type differences. As shown in Figure 2A, integration sites (IS) were identified within all T cell chromosomes with the exception of chromosome Y. This may be due to Y chromosome's relatively smaller size, and would be consistent with the lower number of IS found within relatively smaller chromosomes such as chromosomes 13-22 (Figure 2A and 2B). In contrast to the relatively consistent IS distribution pattern found in T cells derived from two separate donors, several distinct differences were found in integration profile between HEK293 and T cells. For example, in contrast to T cells, no IS were found within chromosome 16 of HEK293 (Figure 2A and 2B). Moreover, a markedly higher percentage of IS were found within chromosomes 5 and 6 of HEK293, whereas more IS were found within chromosome 19 for T cells (from both donors; Figure 2B).

Since *qPB* genome insertion may raise safety concerns, we next analyzed the distribution of IS within or near different areas of genes. A total of 344 and 300 unique IS were identified within T cell donor 1 and donor 2, respectively (Supplementary Table S1). Of note, we observed

that increasing the amount of donor DNA (carrying CAR) introduced into CAR-T cells increases integrant copy number in cells(54). To ensure safety, we optimized the concentration of donor DNA such that integrant copy number per cell would be below five. This is demonstrated here by the low CAR copy numbers found in T cells derived from both donors (3.08 and 1.68 in T cells of donor 1 and 2, respectively; Supplementary Table S1). Interestingly, remarkable conformity was found in the integration profiles of both donor T cells. For example, approximately 50% (50.9% and 52% in cells of donor 1 and donor 2, respectively) of IS were found in the introns, while a very low percentage (0.3% and 1.3% in cells of donor 1 and donor 2, respectively) were found in the open reading frame (ORF) of protein coding gene (Figure 2C). Historical data demonstrated that an even higher percentage (79.7%) of intronic IS found in the lentiviral vector(35) is considered to be relatively safe, suggesting that *qPB* is at least as safe as lentiviral vectors. Moreover, the markedly lower percentage of IS found in the introns (25.2%) and the higher percentage of IS found in the ORF (4.8%) of HEK293 cells further support a cell type-specific distribution of *qPB* IS. Next, we focused on IS in the CpG dinucleotide-rich regions (CpG islands) since the transcription of >50% of human genes are initiated from these regions(36). Lower percentages of IS were found in the regions <= 5 Kb from CpG islands (24.7% and 23.7% in cells of donor 1 and donor 2, respectively) as compared to published data in cells transposed using retrovirus (32.8%) or hyperactive *piggyBac* (26.6%)(35), suggesting *qPB* is potentially safer than both of these vector systems.

Though the majority of IS were identified in genes, none of the top 10 IS of either T cell donors are targeted within cancer-associated genes (Supplementary Table S2). Importantly, while some IS were found in proximity to cancer-associated genes, most were found in the intronic region and IS were found upstream (< 5 Kb) of two such genes (PIK3R2 and MKT2C; Supplementary Table S3). No IS was found in or near any of the genes (CCND2, HMGA2, LMO2, MECOM, MN1) previously reported to be associated with severe adverse events in patients. This distribution pattern of IS is consistent with historical data showing retrovirus, lentivirus, hyperactive *piggyBac* and sleeping beauty IS(35, 37), thereby confirming that *qPB* vector system is at least as safe as any currently available vector systems.

Quantum Nufect™ (*qNF*) facilitates effective transfection of human primary T cells while preserving high cell viability

qNF is a cell type-independent generic buffer system for electroporation. We utilized Lonza's Nucleofector™ to assess the effect of *qNF* on transfection efficiency of human T lymphocytes. We first nucleofected T cells with *qPB* expressing a reporter gene (pmaxGFP) using *qNF*, and compared the results to those obtained using the Human T Cell Nucleofector™ Solution (HTCN, Lonza; Figure 3A). In a representative experiment, unlike the low viability (41%) seen in

HTCN-transfected T cells, *qNF* preserved the viability of a high percentage (96%) of cells at a level comparable to that of non-nucleofected control cells. These results are consistent with a significantly higher viability index in *qNF*- compared to HTCN-nucleofected cells (Figure 3B). We next examined the relationship between cell viability and expansion capacity of T cells transfected with *qPB* using *qNF*. As shown in Figure 3C, initial low viability resulted in lower subsequent expansion after three additional days of culture, suggesting that the higher the cell viability following nucleofection, the greater the capacity for CAR-T expansion.

Next we assessed the effect of *qNF* on CAR transfection efficiency by nucleofecting with *qPB* carrying a bicistronic transcript expressing a tandem CD20/CD19 CAR and iCasp9, using *qNF* or HTCN. As shown in Figure 4A, significantly more total live cells were recovered from the *qNF* group (8.9E5 ± 9.3E4) compared with those recovered from the HTCN group (3.2E5 ± 1.0E5; Figure 4A, 1st panel) one day after nucleofection. While a significantly higher percentage of live cells of the HTCN group were CAR$^+$, there were nearly twice as many CAR$^+$ (and PI$^-$) T cells recovered using *qNF* (2.0E5 ± 3.7E4) compared to that using HTCN (1.2E5 ± 3.8E4; Figure 4A, 2nd and 3rd panels).

Next we addressed whether the greater transfection rate seen in HTCN compared with *qNF* would result in greater percentage of CAR$^+$ cells in the final CAR-T product. We assessed the CAR transfection efficiency using *qNF* in cells obtained from seven healthy donors and compared the results with that obtained from HTCN-nucleofected cells. As shown in Figure 4B, despite an initial lower percentage of CAR$^+$ T cells one day after nucleofection using *qNF*, there was an overall increase in CAR$^+$ cells after 14 days of culture (Figure 3B). This is in contrast to an overall decrease in percentage of CAR$^+$ T cells after 14 days of culture when cells were nucleofected using HTCN. In fact, in cells from five out of seven PBMC donors, the rate (slope) of increase in percentage of CAR$^+$ T cells between one and 14 days following nucleofection was higher in *qNF* than HTCN nucleofected cells (Supplementary Fig. S2). Moreover, in the remaining two donors, the rate of decrease of percentage of CAR$^+$ T cells nucleofected using *qNF* was the same or lower than those nucleofected using the HTCN.

These evidence suggest that higher initial percentage of CAR$^+$ cells do not necessarily translate into better overall enrichment of these cells, and that *qNF* is superior and more reliable in producing and enriching CAR$^+$ T cells than HTCN.

iCellar™ robustly enriches and expands CAR-T cells while maintaining cell stemness (T_{SCM})

We previously showed that *qPB* can be advanced towards clinical application for cancer treatment with CAR-T therapy(53). However, even in the presence of artificial antigen presenting cells (aAPC), T cells from some donors still failed to expand. To resolve this issue, we developed

a CAR-T cell culture supplement, named as *Quantum Booster*™ (*qBT*), which in conjunction with aAPC are both components of *iCellar*™. We then analyzed the effect of *iCellar*™ on performance of CAR-T cells by determining whether different components of *iCellar*™, namely aAPC, *qBT*, or their combination (aAPC+*qBT*), affect the characteristics of CAR-T cells produced. As shown in Figure 5, *qBT* increased the expansion of CAR-T cells (Figure 5A). Furthermore, *qBT* also significantly enriched CAR^+ T cells (Figure 5B). On the other hand, while aAPC does not significantly affect expansion or percentage of CAR^+ T cells, aAPC+*qBT* significantly enhanced both of these parameters (Figure 5A and 5B). Moreover, while either QB or aAPC+*qBT* increased the percentage of T_{SCM} cells over the control group (Figure 5C and 5D, respectively), aAPC alone markedly decreased the percentage of T_{SCM} cells. This effect, which reached statistical significance in the $CD8^+$ population (Figure 5D) suggests that aAPC promotes cell maturation. Furthermore, aAPC+*qBT* significantly blocked the reduction in percentage of T_{SCM} cells (Figure 5C and 5D), suggesting that *qBT* maintains cells in a less differentiated state (i.e. T_{SCM}). These results demonstrate that *qBT* of *iCellar*™ markedly and universally enhance the expansion capacity of CAR-T cells while preserving and/or even enhancing CAR-T quality.

Effective tumor clearance by *qCART*™ system-derived CAR-T cells in Raji-bearing immunodeficient mice

To further determine the effect of aAPC on the functionality of *qCART*™-derived CAR-T cells, we characterized the *in vitro* and *in vivo* cytotoxicity of CAR-T cells. We first assessed the performance of CAR-T production in T cells from four healthy donors (Supplementary Table S4). We found similar and consistent performance in cells from all four donors, and assessed cytotoxic activities in T cells from donor A. CAR-T cells effectively lysed cultured Raji-GFP/Luc target cells (Figure 6A). CAR-T cells expanded with aAPC also significantly increased their killing efficacy at earlier (24h and 48h) time points. In contrast to vehicle and pan-T cell-injected mice, Raji-bearing mice injected with CAR-T cells (cultured with either *qBT* or *qBT*+aAPC) for 14 days killed markedly more Raji tumor cells (Figure 6B, 6C), despite the significantly higher plasma levels of IFN-γ in mice injected with pan-T cells (Supplementary Fig. S3A, see day 15). Moreover, preincubation of CAR-T cells with *qBT*+aAPC led to more rapid plasma IFN-γ increase, which subsequently dropped to baseline levels (Supplementary Fig. S3A). The superior antitumor efficacy of CAR-T cells either with *qBT* or *qBT*+aAPC was also shown by the prolonged survival of these mice compared with those injected with vehicle or pan-T cells (Figure 6D). This observation is consistent with the absence of detectable Raji cells remaining in the blood and bone marrow of CAR-T treated mice (either with *qBT* or *qBT*+aAPC) for 85 days (Supplementary Fig. S3C). Interestingly, we observed tumor relapse in mice that had been injected with CAR-T cells cultured with *qBT*+aAPC, but not with *qBT* alone. We also observed that in one mouse (first

mouse from the left in the "CAR-T (*qBT*)" panel) tumor relapsed by day 21, however, complete tumor remission was again observed by day 34 with no evidence of relapse up to 83 days following CAR-T injection (Figure 6B). This observation together with the higher number of CAR^+ T cells (indicated by the relatively higher CAR copies per ng of blood cells) found in mice injected with CAR-T cells (with QB or QB+aAPC) on day 71 as compared to that found on day 43 (Supplementary Fig. S3B), suggest that the increase in CAR^+ T cells contribute to tumor clearance.

qCART™ produces CAR-T cells of different targeting specificity and gene of interest sizes with expansion capacity capable of reaching clinical scale production

To determine whether CAR-T cells with different CAR genes expressing binder(s) against various antigens and/or transgene of various sizes could be effectively generated, we nucleofected *qPB* carrying various transgenes of interest into T cells obtained from healthy donors and analyzed the resulting CAR-T cell characteristics. Increasing the transgene size decreased the percentage and expansion capacity of CAR-T cells (Table 2). No obvious effect of transgene size on the percentage of T_{SCM} cells in the $CD4^+$ or $CD8^+$ T cell subtypes was observed. Notably, the T_{SCM} subset remains the major population in both subtypes. Furthermore, in a ten-day culture, *iCellar*™ facilitates the production of clinical scale (up to 10e9) CAR^+ T_N/T_{SCM} cells in one liter of culture (calculated from Fig. 5). Together, these results demonstrate that irrespective of gene identity and size, T cell production performance using *qCART*™ is still within satisfactory range. It also lends support to the feasibility of producing multiplexed CAR-T cells for clinical application.

Discussion

The success of CAR-T therapy in treating liquid cancer has not been replicated in solid tumor(38–40). In this study, we demonstrated that *qCAR-T*™ is a simple, economic, and robust virus-free cell engineering system that expedites the development and manufacturing of next-generation, virus-free multiplex CAR-T therapy.

The lack of cancer-specific antigen and the immunosuppressive tumor microenvironment in solid tumors presents a major challenge. One strategy to overcome these obstacles is to engineer T cells to simultaneously express multiple therapeutic genes in individual cells. This can only be achieved using a technology capable of performing one-step multiplex gene integration in a single cargo. Given the complexity of solid tumors and the distinct attributes for each cancer type, a library of CAR-T cells with a large repertoire of GOI designs can be used to identify the most effective and safest gene design. Furthermore, a system for rapidly assessing the targeting

specificity and On-Target Off-Tumor toxicities of CAR-T cells is urgently needed. Lastly, high-throughput cytotoxicity assays are required to identify the most efficacious and persistent CAR-T cells. *GTailor*™, the R&D component of the *qCART*™ system, addresses all of the aforementioned needs. It is used to streamline the identification process for the most optimal multiplex gene design that can be tailored to combat a wide-spectrum of cancers.

Production and product consistencies are the most desirable manufacturing attributes. By applying the *qCART*™ system in small-scale CAR-T cell production, we routinely obtain high quality CAR-T products with low batch and donor discrepancies. Thus, *GTailor*™ may be considered a miniature version of *qCART*™ that can be used to fine tune the CAR-T cell production process. It can be readily scaled up to clinical quantity without extensive optimizing steps. The four *qCART*™ platforms achieve consistencies in two parts. The first is the effectiveness of transfection, chromosomal transposition, and CAR-T cell expansion during the CAR-T cell production process. The second includes all of the desired features of a CAR-T product: safety, identity, purity, and potency. CD19/CD20 tandem CAR-T with iCasp9 product is a sample product that possesses all of these desired features(54). Possible mechanisms that contribute to the desirable high CAR-T_{SCM}, high CD8:CD4 ratio, and minimal safety concerns are discussed below.

A transfection reagent capable of achieving high-efficiency gene delivery with minimal toxicity is imperative for producing reliable gene-modified cell products. Compared to HTCN, electroporation of $CD3^+$ T cells using *qNF* is a gentler method and resulted in higher CAR-T cell production 14 days after culture (Figure 3 and 4). The observed discrepancy in CAR-T cell production can be explained by differential transient transgene expression. Unlike the skewed, high CAR expression in HTCN-transfected T cells (Figure 3A), CAR expression profile in the *qNF* is distributed evenly across a wide spectrum. An excess of DNA contributed to cellular toxicity(41). Thus, the skewed high level of transient CAR expression in HTCN-transfected T cells may have caused greater cellular toxicity, reducing cell survival and subsequent CAR-T expansion. Activation-induced cell death (AICD) resulting from repeated T-cell receptor activation may also play a role (42). It is possible that the skewed high level CAR expression caused the leaky activation of 4-1BB signals to reach a threshold level capable of triggering AICD in the HTCN-transfected CAR^-T cells, resulting in a decline in percentage of CAR^+ cells (Figure 4 and Figure S2). On the contrary, the wide-spectrum CAR expression level in *qNF*-transfected cells may result in: (1) greater CAR-T cell survival due to reduced AICD and/or electroporation-induced death and (2) greater CAR^+ T cell expansion due to lower cell damage after electroporation. The lower transfection rate by *qNF* as compared to HTCN is rescued by *qPB*'s superior gene integration efficiency. Thus, the two platforms coordinate with each other to further enrich CAR^+ T cell population in CAR-T product.

Risks associated with random gene integration represent a major safety concern in gene therapy. A recent clinical report demonstrated that two of 10 patients treated with *piggyBac*-modified CD19 CAR-T therapy developed CAR-T-cell lymphoma(43). A detailed mechanistic study on the case reveals a high number of *piggyBac* integrants, but none were inserted to or near typical oncogenes(44). This study highlights the importance of keeping a low copy number of integrants per genome in gene therapy products. Our previous study has demonstrated that *qPB* is the most effective *piggyBac*-based transposon system for engineering CAR-T cells(53). Here, we have further confirmed that *qPB* is a potentially safe vector for producing clinical-grade CAR-T cells given its low copy number of integrant (<5 copies per cell) and safe genome-wide integration profile in CAR-T products. Furthermore, as compared to hyperactive *piggyBac*, *qPB* leaves behind significantly lower amount of backbone residues (107 bp vs. ~600 bp) on the genome that lacks the dominant enhancer activity found in backbone residues of hyperactive *piggyBac*, thereby making it a relatively safer *piggyBac* system(53) for CAR-T cell production.

Naïve T cells (T_N) and T_{SCM} have the capacity to persist and proliferate long-term in cancer patients, leading to improved clinical outcome(45). Hence, enriching these cell types, especially CAR^+ T_{SCM} cells, has become a central focus in the development of next-generation CAR-T therapy(28–31). Our studies have demonstrated that almost all *qCART*™-generated CAR-T cell products contain >90% T_N and T_{SCM} (> 70% T_{SCM} in most cases) in both CD4 CAR^+ and CD8 CAR^+ T cell populations, regardless of (1) CAR construct design, (2) GOI size, and (3) PBMC source (healthy donors or patients with B-cell malignancies) (Figure 5, Table 2, and paper 3). We believe this desired feature is synergistically achieved by the combined benefits derived from: (1) including 4-1BB rather than CD28 in our CAR construct, (2) using *qNF* (GenomeFrontier) instead of HTCN (Lonza) for nucleofection, (3) choosing virus-free *qPB* over viral or other virus-free vector systems (e.g. hyperactive *piggyBac*), and (4) using *iCellar*™, *qBT* in particular, for CAR-T cell expansion. The following are the possible mechanisms that may contribute to the high CAR-T_{SCM} enrichment in our CAR-T products. First, it has been demonstrated that 4-1BB signaling in CAR-T cells promotes T_{SCM} expansion, whereas CD28 favors T_{EFF} expansion(46). Second, as shown in Figure 3C, the greater the electroporation-induced cell damage, the lower the cell expansion capacity. It is highly likely that degree of electroporation-induced damage is further amplified in highly proliferating cells (e.g. T_{SCM}). Third, extended *ex vivo* expansion of viral CAR-T cells often results in a more differentiated T_{EFF} phenotype with higher expression of exhaustion markers, such as TIM3 and PD1. In contrast, *piggyBac*-based CAR-T products consistently have T_{SCM} as their major population when cells are *ex vivo*-cultured in the same time frame, which may be further strengthened by applying *qPB* rather than hyperactive *piggyBac* as a genetic tool. Finally, current *ex vivo* approaches to expand CAR-T cells to sufficient numbers while maintaining a minimally-differentiated phenotype are

hindered by the biological coupling of clonal expansion and effector differentiation. In this study we demonstrated that *qBT*, a component of *iCellar*™, not only promoted robust CAR-T cell expansion but also maintained T cell stemness even in the presence of antigen-expressing aAPC. *qBT* likely accomplished this by increasing the CD4 CAR^+ T_{SCM} population (Figure 5C). Consequently, these CD4 T cells may enhance proliferation of CD8 T_{SCM} population without concomitant differentiation. This in turn may result in high (3-9) and balanced (approximately 1)(54). CD8:CD4 ratios in healthy donors and patients, respectively. Our recent study further confirms that the *qCART*™-derived CAR-T products (derived from either healthy or B-cell malignant patient PBMC) contain limited senescent or exhausted T cells, as only a small percentage of the cell population expresses these markers.

Since the publication of first clinical studies in 2016(47), it has been thought that healthy T cell-derived allogeneic CAR-T therapies, the so called “off-the-shelf” CAR-T products, will inevitably replace autologous CAR-T products. However, ample clinical data have concluded that allogeneic CAR-T products are less potent and limited in CAR-T cell persistence as compared to their autologous counterpart. In October 2021, the FDA placed a clinical hold on all Allogene Therapeutics’ AlloCAR-T clinical trials after a chromosomal abnormality was found in a patient who received the anti-CD19 allogeneic CAR-T therapy. The incident further raised concerns regarding all allogeneic CAR-T therapies, impeding development of this type of therapy. Induced pluripotent stem cells (iPSC)-derived CAR-T cells may be a promising alternative for allogeneic CAR-T therapy. However, such approaches are at an early stage in development and require further pre-clinical and clinical studies. Furthermore, the heavy mutation burden of iPSCs poses safety concerns for its clinical applications. Thus, autologous CAR-T therapy is likely to remain the mainstay of CAR-T based treatments, at least in the short to medium term. In this study, we demonstrated that the *qCART*™ system provides the solution to most if not all of the current challenges of autologous CAR-T therapy. Thus, this simple, robust, and virus-free *qCART*™ system will likely set a new paradigm in the CAR-T field.

Materials and Methods

Human T cell samples from healthy donors

Blood samples from adult healthy donors were obtained from Chang Gung Memorial Hospital (Linkou, Taiwan), the acquisition of these samples was approved by the Institution Review Board (IRB No. 201900578A3) at Chang Gung Medical Foundation.

GTailor™ identification of lead candidates

A proprietary collection of primary cells and (engineered and non-engineered) cell lines were used for *in vitro* evaluation of ON-Target anti-tumor activities. Cancer cell lines were engineered

with a construct expressing green fluorescence protein or tdTomato reporter gene, with or without co-expression of luciferase gene. Stable lines were generated using either a *piggyBac* or a lentivirus vector system. With regards to constructs, a collection composed of parental plasmids of various configurations were used to generate a library of constructs, and the indicated gene(s) of interest (GOI) of various identities and sizes were cloned into the vector's multiple cloning site. *qPB* parental donor plasmids carrying the indicated GOI were used to construct minicircle DNA using methodology as previously described(48). CAR-T cells produced by nucleofection with these donor constructs in combination with a Quantum pBase helper plasmid (i.e. *qPB*) were evaluated for their performance as well as their ability to mediate *in vitro* cytotoxicity against the collection of cells. When a lead candidate is identified, its *in vivo* antitumor activity is also evaluated in a mouse xenograft model.

Mapping of *Quantum pBac*™ genome integration sites (IS)

Genomic DNA of CAR-T products was extracted using DNeasy Blood and Tissue Kit (QIAGEN) and randomly fragmented using a Bioruptor® Pico sonication device (Diagenode) to form fragments of <500 bp. The fragments were ligated to adapters, purified by AMPure XP beads (Beckman Coulter), and amplified by performing nine cycles of PCR reactions. The amplified products with an end sequence of the CAR gene were captured and further amplified by PCR. The final PCR products were subjected to sequencing using NovaSeq system (Illumina) with a 2x150 paired-end configuration setting.

Following sequencing, the raw reads sequencing data were processed using the Agilent Genomics NextGen Toolkit (AgeNT) software module (Agilent) to remove adapter and molecular barcode sequences. The reads were then aligned to the hg38 human genome using Burrows–Wheeler aligner (version 0.7.17-r1188)(49) and the mapping results sorted using SAMtools (version 1.9)(50). IS were manually identified with the assistance of Genome Rearrangement Identification Software Suite (GRIDSS)(51) and BEDTools (version 2.30.0)(51). For analysis of IS in proximity to cancer-associated genes, reads data was compared with cancer gene database downloaded from Cancer Hotspots (https://www.cancerhotspots.org/).

Generation and expansion of CAR-T cells

Peripheral blood mononuclear cells (PBMCs) were isolated from blood samples of healthy donors by utilizing Ficoll-Hypaque gradient separation. $CD3^+$ T cells were isolated from PBMCs using EasySep™ Human T Cell Isolation Kit (StemCell Technologies) according to the manufacturer's instructions. T cells were activated by co-incubation with Dynabeads™ (Invitrogen) for two days at a beads to cells ratio of 3:1. Following the removal of Dynabeads™, activated T cells were subjected to Nucleofection with a CAR transposon minicircle and a Quantum pBase™ plasmid

using a Nucleofector™ 2b or 4D Device (Lonza) in combination with either the Amaxa® Human T Cell Nucleofector® Kit (Lonza) or the *qNF* Kit (GenomeFrontier), as according to the respective manufacturer's instructions. In experiments assessing the effect of cell viability on expansion capacity, T cells were nucleofected using different program settings on the Nucleofector™ 2b Device and cultured for four days in OpTmizer medium (Thermo Fisher Scientific) supplemented with 50IU of IL-2 (PeproTech) and 10% FBS (Caisson). In experiments involving the addition of aAPC, γ-irradiated aAPC were added on Day 3 to T cells at a 1:1 aAPC:T cell ratio. T cells with or without addition of aAPC were cultured in OpTmizer medium, supplemented with 50IU of IL-2 and 10% FBS or *qBT* (GenomeFrontier). On day 12 (aAPC rechallenge experiments), aAPC were added to cells and co-cultured with the T cells until harvesting at 28 days.

Evaluation of CAR-T cell performance

CAR expression on T cells was determined by staining cells at 4℃ for 30 minutes with F(ab')□ fragment specific, biotin-conjugated goat anti-mouse antibodies (Jackson ImmunoResearch Laboratories), and R-phycoerythrin (PE)-conjugated streptavidin (Jackson ImmunoResearch Laboratories). Similarly, cells were also stained with the following antigen-specific antibodies: CD3-Pacific Blue, CD4-Alexa Flour 532 (Thermo Fisher Scientific), CD8-PE-Cy7, CD45RA-BV421, CD62L-PE-Cy5, or CD95-BV711 (Biolegend). Cells may also be incubated with propidium iodide (PI, Thermo Fisher Scientific) and/or Acridine orange (AO, Nexcelom). PI^- cells and T cell differentiation subsets were determined by flow cytometry based on CD45RA, CD62L and CD95 expression: T_N ($CD45RA^+CD62L^+CD95^-$), T_{SCM} ($CD45RA^+CD62L^+CD95^+$), T_{CM} ($CD45RA\text{-}CD62L^+$), T_{EM} ($CD45RA\text{-}CD62L^-$), and T_{EFF} ($CD45RA^+CD62L^-$). Flow cytometric measurements and analyses were performed on a SA3800 Spectral Analyzer (Sony). Histograms and dot-plots were generated using GraphPad Prism software (GraphPad). Total day 1 live cells were determined using Celigo image cytometry (Nexcelom) and represent the number of AO^+, PI^- cells. Viability index was calculated according to the formula: (AO^+, PI^- live cells on day 1/total number of electroporated cells) x 100. Number of CAR^+ live cells was calculated according to the formula: Total day 1 live cells x percentage of CAR^+ of live cells.

***In vivo* cytokine release assay**

Mouse serum samples were collected on Days 3, 15, 29 and 43 following T cell injection. The serum levels of interferon gamma (IFN-γ) was measured by performing enzyme-linked immunosorbent assay (Thermo Fisher) according to the manufacturer's instructions.

***In vitro* cytotoxicity assay**

5 x 10^3 cells per well of Raji-GFP/Luc target cells were seeded in 96-well culture plates (Corning) and CAR-T cells were added at an E:T ratio of 1:1. CAR-T cell mediated cytotoxicity on Raji-GFP/Luc target cells was then assessed by using Celigo image cytometry (Nexcelom) to determine the number of live Raji-GFP/Luc cells at 0, 24, 48, 72 and 96 hours after co-culturing. Cell aggregates were separated by pipetting before Celigo imaging. The percent specific lysis for each sample was calculated using the formula: [1-(live fluorescent cell count in the presence of Raji-GFP/Luc cells and CAR-T cells / live fluorescent cell count in the presence of Raji-GFP/Luc cells only)] x 100.

Mouse xenograft model

In vivo studies using mouse xenograft model were conducted at the Development Center for Biotechnology, Taiwan, using animal protocols approved by the Taiwan Mouse Clinic IACUC (2020-R501-035). Briefly, eight-week-old female ASID (NOD.Cg-Prkdc^{scid}Il2rg^{tm1Wjl}/YckNarl) mice (National Laboratory Animal Center, Taiwan) were intravenously (i.v.) injected with 1.5□×□10^5 Raji-Luc/GFP tumor cells. One week after Raji-Luc/GFP tumor cell injection, mice were injected with 3 x 10^6 CAR-T cells or control Pan-T cells. Luminescence signals from Raji-Luc/GFP tumor cells was monitored using the Xenogen-IVIS Imaging System (Caliper Life Sciences).

Genomic DNA extraction and quantitative PCR (qPCR)

Genomic DNA from mouse blood was extracted using DNeasy Blood & Tissue Kit (Qiagen) following the manufacturer's instructions. A 7500 fast real-time PCR system (Applied Biosystems) was used to carry out quantitative PCR analysis. The amplification of CAR gene (CAR-T cells) and Luc gene (Raji-GFP/Luc cells) in mouse blood samples was carried out using the CAR forward primer (5'-ACGTCGTACTCTTCCCGTCT-3'), CAR reverse primer (5'-GATCACCCTGTACTGCAACCA-3') and the luciferase forward primer (5'-GGACTTGGACACCGGTAAGA-3') and luciferase reverse primer (5'-GGTCCACGATGAAGAAGTGC-3'), respectively. The amount of CAR and Luc gene, expressed as gene copy/ng of DNA, were calculated utilizing the standard curve method as previously described.(52)

Statistical analysis

Statistical analyses of differences between two groups and among three or more groups were carried out using the Student's t-test (two-tailed) and the one-way ANOVA with Tukey's multiple comparison test, respectively. The analyses were performed using Prism 7.0 (GraphPad), and statistical significance was reported as * $p < 0.05$, ** $p < 0.01$, and *** $p < 0.001$.

Acknowledgments

The authors thank Ms. Yi-Shan Yu and Ms. Lu-Chun Chen for their assistance throughout the IRB preparation and approval process. The authors also thank Dr. Pei-Yi Tsai for assistance with the animal experiments.

References

1. S. Akkın, G. Varan, E. Bilensoy, A review on cancer immunotherapy and applications of nanotechnology to chemoimmunotherapy of different cancers. *Molecules* **26** (2021).

2. A. D. Waldman, J. M. Fritz, M. J. Lenardo, A guide to cancer immunotherapy: from T cell basic science to clinical practice. *Nature Reviews Immunology* **20** (2020).

3. J. N. Brudno, *et al.*, T cells genetically modified to express an anti–B-Cell maturation antigen chimeric antigen receptor cause remissions of poor-prognosis relapsed multiple myeloma. *Journal of Clinical Oncology* **36** (2018).

4. M. Alexander, *et al.*, Chimeric Antigen Receptor T Cell Therapy: A Comprehensive Review of Clinical Efficacy, Toxicity, and Best Practices for Outpatient Administration: M. Alexander et al. *Transplantation and Cellular Therapy* **27** (2021).

5. A. I. Salter, M. J. Pont, S. R. Riddell, Chimeric antigen receptor-modified T cells: CD19 and the road beyond. *Blood* **131** (2018).

6. S. P. D'angelo, *et al.*, Antitumor activity associated with prolonged persistence of adoptively transferred NY-ESO-1c259T cells in synovial sarcoma. *Cancer Discovery* **8** (2018).

7. N. Raje, *et al.*, Anti-BCMA CAR T-Cell Therapy bb2121 in Relapsed or Refractory Multiple Myeloma. *New England Journal of Medicine* **380** (2019).

8. M. Kalos, *et al.*, T cells with chimeric antigen receptors have potent antitumor effects and can establish memory in patients with advanced leukemia. *Science Translational Medicine* **3** (2011).

9. R. Mohanty, *et al.*, CAR T cell therapy: A new era for cancer treatment (Review). *Oncology Reports* **42** (2019).

10. S. Srivastava, S. R. Riddell, Engineering CAR-T cells: Design concepts. *Trends in Immunology* **36** (2015).

11. B. Savoldo, *et al.*, CD28 costimulation improves expansion and persistence of chimeric antigen receptor-modified T cells in lymphoma patients. *Journal of Clinical Investigation* **121** (2011).

12. E. Bôle-Richard, *et al.*, CD28/4-1BB CD123 CAR T cells in blastic plasmacytoid dendritic cell neoplasm. *Leukemia* **34** (2020).

13. H. Zhang, *et al.*, 4-1BB Is Superior to CD28 Costimulation for Generating CD8 + Cytotoxic Lymphocytes for Adoptive Immunotherapy . *The Journal of Immunology* **179** (2007).

14. A. H. Long, *et al.*, 4-1BB costimulation ameliorates T cell exhaustion induced by tonic signaling of chimeric antigen receptors. *Nature Medicine* **21** (2015).

15. K. M. Cappell, J. N. Kochenderfer, A comparison of chimeric antigen receptors containing CD28 versus 4-1BB costimulatory domains. *Nature Reviews Clinical Oncology* **18** (2021).

16. S. Li, *et al.*, Treatment of acute lymphoblastic leukaemia with the second generation of CD19 CAR-T containing either CD28 or 4-1BB. *British Journal of Haematology* **181** (2018).

17. F. Marofi, *et al.*, CAR T cells in solid tumors: challenges and opportunities. *Stem Cell Research and Therapy* **12** (2021).

18. U. Patel PharmD, *et al.*, CAR T cell therapy in solid tumors: A review of current clinical trials (2021) https:/doi.org/10.1002/jha2.356.

19. Z. zheng Zhang, *et al.*, Improving the ability of CAR-T cells to hit solid tumors: Challenges and strategies. *Pharmacological Research* **175** (2022).

20. O. O. Yeku, T. J. Purdon, M. Koneru, D. Spriggs, R. J. Brentjens, Armored CAR T cells enhance antitumor efficacy and overcome the tumor microenvironment. *Scientific Reports* **7** (2017).

21. E. R. Hawkins, R. R. D'souza, A. Klampatsa, Armored CAR T-cells: The next chapter in T-cell cancer immunotherapy. *Biologics: Targets and Therapy* **15** (2021).

22. K. Adachi, *et al.*, IL-7 and CCL19 expression in CAR-T cells improves immune cell infiltration and CAR-T cell survival in the tumor. *Nature Biotechnology* **36** (2018).

23. J. T. Zhou, *et al.*, EGLIF-CAR-T cells secreting PD-1 blocking antibodies significantly mediate the elimination of gastric cancer. *Cancer Management and Research* **12** (2020).

24. Y. Ping, *et al.*, Augmenting the Effectiveness of CAR-T Cells by Enhanced Self-Delivery of PD-1-Neutralizing scFv. *Frontiers in Cell and Developmental Biology* **8** (2020).

25. E. R. Suarez, *et al.*, Chimeric antigen receptor T cells secreting anti-PD-L1 antibodies more effectively regress renal cell carcinoma in a humanized mouse model. *Oncotarget* **7** (2016).

26. B. D. Choi, *et al.*, CAR-T cells secreting BiTEs circumvent antigen escape without detectable toxicity. *Nature Biotechnology* **37** (2019).

27. L. Gattinoni, *et al.*, A human memory T cell subset with stem cell-like properties. *Nature Medicine* **17** (2011).

28. S. Arcangeli, *et al.*, Next-Generation Manufacturing Protocols Enriching TSCM CAR T Cells Can Overcome Disease-Specific T Cell Defects in Cancer Patients. *Frontiers in Immunology* **11** (2020).

29. M. Zhang, *et al.*, Optimization of metabolism to improve efficacy during CAR-T cell manufacturing. *Journal of Translational Medicine* **19** (2021).

30. C. Fu, G. Shi, Y.-T. Liu, Manufacturing Anti-CD19 CAR-Tscm Cells for Immunotherapy Using Innovative Microbubble-Based Technologies for Precision Cell Processing. *Blood* **138** (2021).

31. C. Ronald Funk, *et al.*, "PI3Kd/g inhibition promotes human CART cell epigenetic and metabolic reprogramming to enhance antitumor cytotoxicity" (2022) https:/doi.org/10.1182/blood.2019000962.

32. R. A. Morgan, B. Boyerinas, Genetic modification of T cells. *Biomedicines* **4** (2016).

33. J. T. Bulcha, Y. Wang, H. Ma, P. W. L. Tai, G. Gao, Viral vector platforms within the gene therapy landscape. *Signal Transduction and Targeted Therapy* **6** (2021).

34. Y. J. J. Meir, *et al.*, A versatile, highly efficient, and potentially safer piggyBac transposon system for mammalian genome manipulations. *FASEB Journal* **27**, 4429–4443 (2013).

35. M. Hamada, *et al.*, Integration Mapping of piggyBac-Mediated CD19 Chimeric Antigen Receptor T Cells Analyzed by Novel Tagmentation-Assisted PCR. *EBioMedicine* **34**, 18–26 (2018).

36. T. Vavouri, B. Lehner, Human genes with CpG island promoters have a distinct transcription-associated chromatin organization. *Genome Biology* **13** (2012).

37. Kebriaei P, *et al.*, The Journal of Clinical Investigation (2016) https:/doi.org/10.1172/JCI86721.

38. F. C. Thistlethwaite, *et al.*, The clinical efficacy of first-generation carcinoembryonic antigen (CEACAM5)-specific CAR T cells is limited by poor persistence and transient pre-conditioning-dependent respiratory toxicity. *Cancer Immunology, Immunotherapy* **66** (2017).

39. C. H. J. Lamers, *et al.*, Treatment of metastatic renal cell carcinoma with CAIX CAR-engineered T cells: Clinical evaluation and management of on-target toxicity. *Molecular Therapy* **21** (2013).

40. C. E. Brown, *et al.*, Bioactivity and safety of IL13Rα2-redirected chimeric antigen receptor CD8+ T cells in patients with recurrent glioblastoma. *Clinical Cancer Research* **21** (2015).

41. S. Huerfano, B. Ryabchenko, J. Forstová, Nucleofection of expression vectors induces a robust interferon response and inhibition of cell proliferation. *DNA and Cell Biology* **32**, 467–479 (2013).

42. D. R. Green, N. Droin, M. Pinkoski, Activation-induced cell death in T cells. *Immunological Reviews* **193** (2003).

43. D. C. Bishop, *et al.*, Development of CAR T-cell lymphoma in 2 of 10 patients effectively treated with piggyBac-modified CD19 CAR T cells. *Blood* **138** (2021).

44. K. P. Micklethwaite, *et al.*, Investigation of product-derived lymphoma following infusion of piggyBac-modified CD19 chimeric antigen receptor T cells. *Blood* **138** (2021).

45. J. A. Fraietta, *et al.*, Determinants of response and resistance to CD19 chimeric antigen receptor (CAR) T cell therapy of chronic lymphocytic leukemia. *Nature Medicine* **24** (2018).

46. O. U. Kawalekar, *et al.*, Distinct Signaling of Coreceptors Regulates Specific Metabolism Pathways and Impacts Memory Development in CAR T Cells. *Immunity* **44** (2016).

47. J. N. Brudno, *et al.*, Allogeneic T cells that express an anti-CD19 chimeric antigen receptor induce remissions of B-cell malignancies that progress after allogeneic hematopoietic stem-cell transplantation without causing graft-versus-host disease. *Journal of Clinical Oncology* **34** (2016).

48. M. A. Kay, C. Y. He, Z. Y. Chen, A robust system for production of minicircle DNA vectors. *Nature Biotechnology* **28**, 1287–1289 (2010).

49. H. Li, Aligning sequence reads, clone sequences and assembly contigs with BWA-MEM (2013).

50. H. Li, *et al.*, The Sequence Alignment/Map format and SAMtools. *Bioinformatics* **25** (2009).

51. D. L. Cameron, *et al.*, GRIDSS: Sensitive and specific genomic rearrangement detection using positional de Bruijn graph assembly. *Genome Research* **27** (2017).

52. X. Zhou, *et al.*, Preclinical safety evaluation of recombinant adeno-associated virus 2 vector encoding human tumor necrosis factor receptor-immunoglobulin Fc fusion gene. *Human Vaccines and Immunotherapeutics* **12** (2016).

53. W.-K. Hua, et al., *Quantum pBac*: An effective, high-capacity *piggyBac*-based gene integration vector system for unlocking gene therapy potential. (*Manuscript in preparation*).

54. Y.-C. Chen, et al., Manufacturing highly potent CD20/CD19-targeted iCasp9 regulatable CAR-T cells using the *Quantum pBac*-based CAR-T (*qCART*™) system for clinical application. (*Manuscript in preparation*).

Figures and Tables

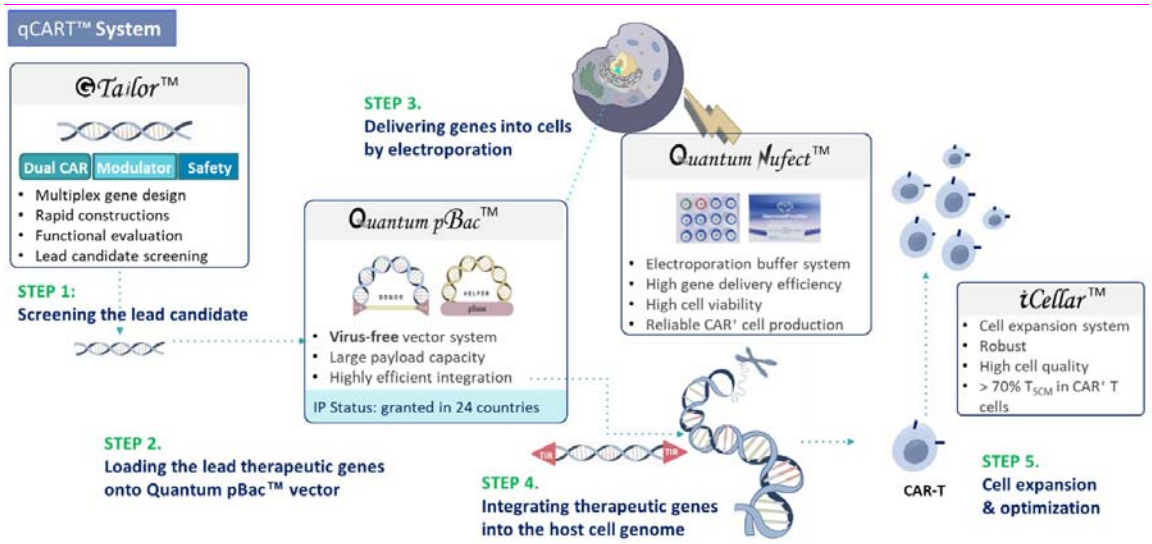

Figure 1. The *qCART*™ system

A schematic depiction showing the components of the *qCART*™ system.

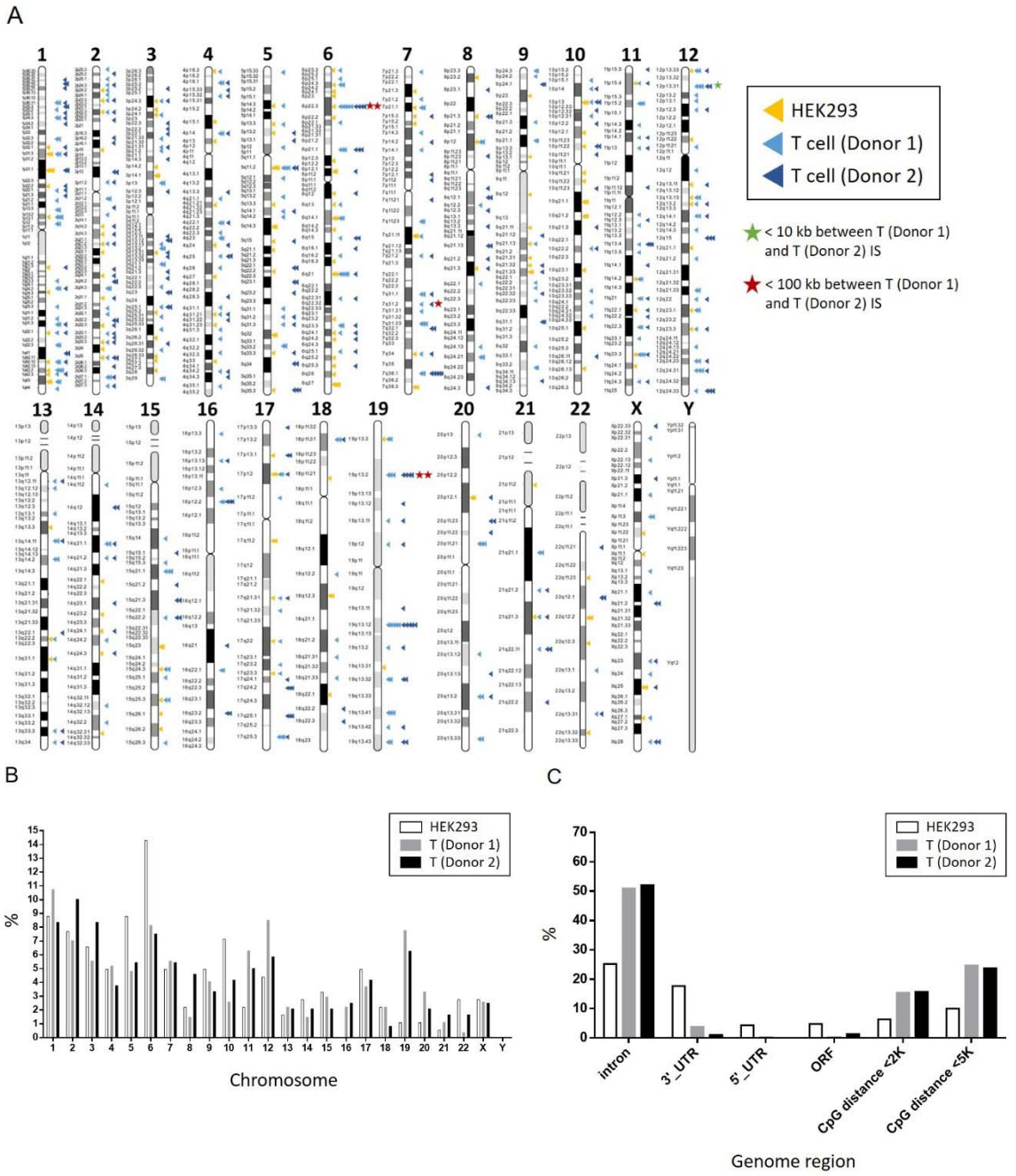

Figure 2. Profiling of *Quantum pBac*™ (*qPB*) genome integration

(A) A schematic depiction showing the distribution of *qPB* genome integration sites (IS) mapping to specific segments of the indicated HEK293 and primary T cell chromosomes. (B), (C) IS as shown in (A), data analyzed and grouped by: the indicated chromosome (B), and the indicated genome region (C). Results shown are from two females (HEK293, T donor 2) and one male (T donor 1), and results of (B) and (C) are presented as percentages of total IS.

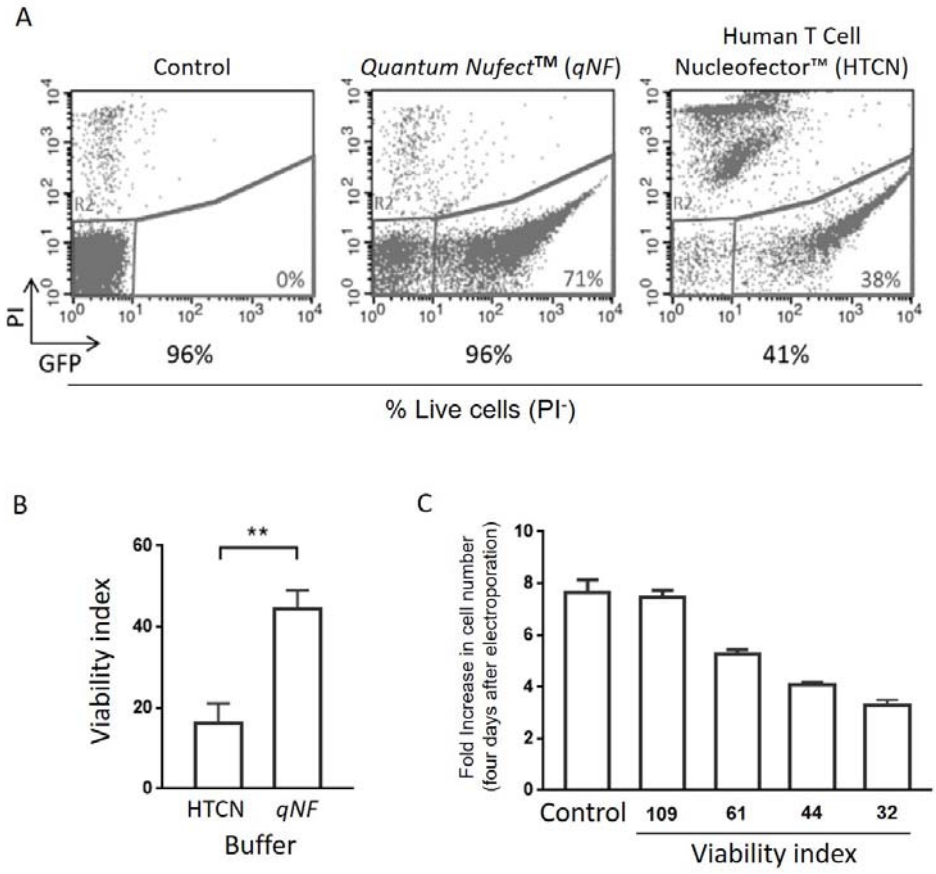

Figure 3. Viability of human primary T cells electroporated using *Quantum Nufect*™ (*qNF*) buffer system compared with those electroporated using the Human T Cell Nucleofector™ solution

Human peripheral blood T cells electroporated with *Quantum pBac*™ expressing pGFPmax in either *qNF* buffer or Human T Cell Nucleofector™ (HTCN) solution were harvested one day after electroporation and analyzed for (A) GFP and PI staining, and (B) viability index. (C) Human peripheral blood T cells electroporated under conditions that result in different levels of post-electroporation viability were analyzed for their viability indices plotted versus fold increase in cell number after four days of culture. Results are shown as percentage of cells positive or not positive for GFP and/or PI staining (A), mean viability index (B, C) and the mean fold increase in number of cells (C). ** $p < 0.01$. N = 3 (B, C, triplicates).

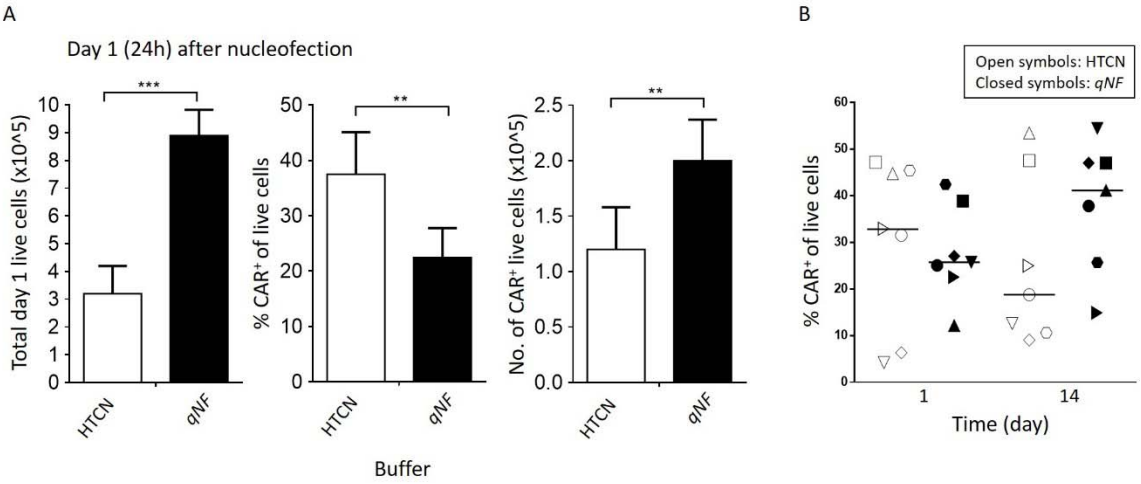

Figure 4. Higher yield of CAR$^+$ T cells obtained from human primary T cells electroporated using *Quantum Nufect*™ (*qNF*) buffer system compared with those electroporated using the Human T Cell Nucleofector™ (HTCN) solution

Human peripheral blood T cells electroporated with *Quantum pBac*™ expressing CAR in either *qNF* buffer or HTCN solution were harvested one day after electroporation and analyzed for (A) CAR and PI staining, and yield calculation. (B) The percentages of CAR$^+$ cells were analyzed on day 1 and day 14. Results are shown in (B) as median percentage of CAR$^+$ live cells. Yield is calculated as No. of CAR$^+$ live cells, using the formula: (Total day 1 live cells) × (percentage of CAR$^+$ live cells). ** $p < 0.01$, *** $p < 0.001$. N = 3 (A, triplicates), N = 7 donors (B).

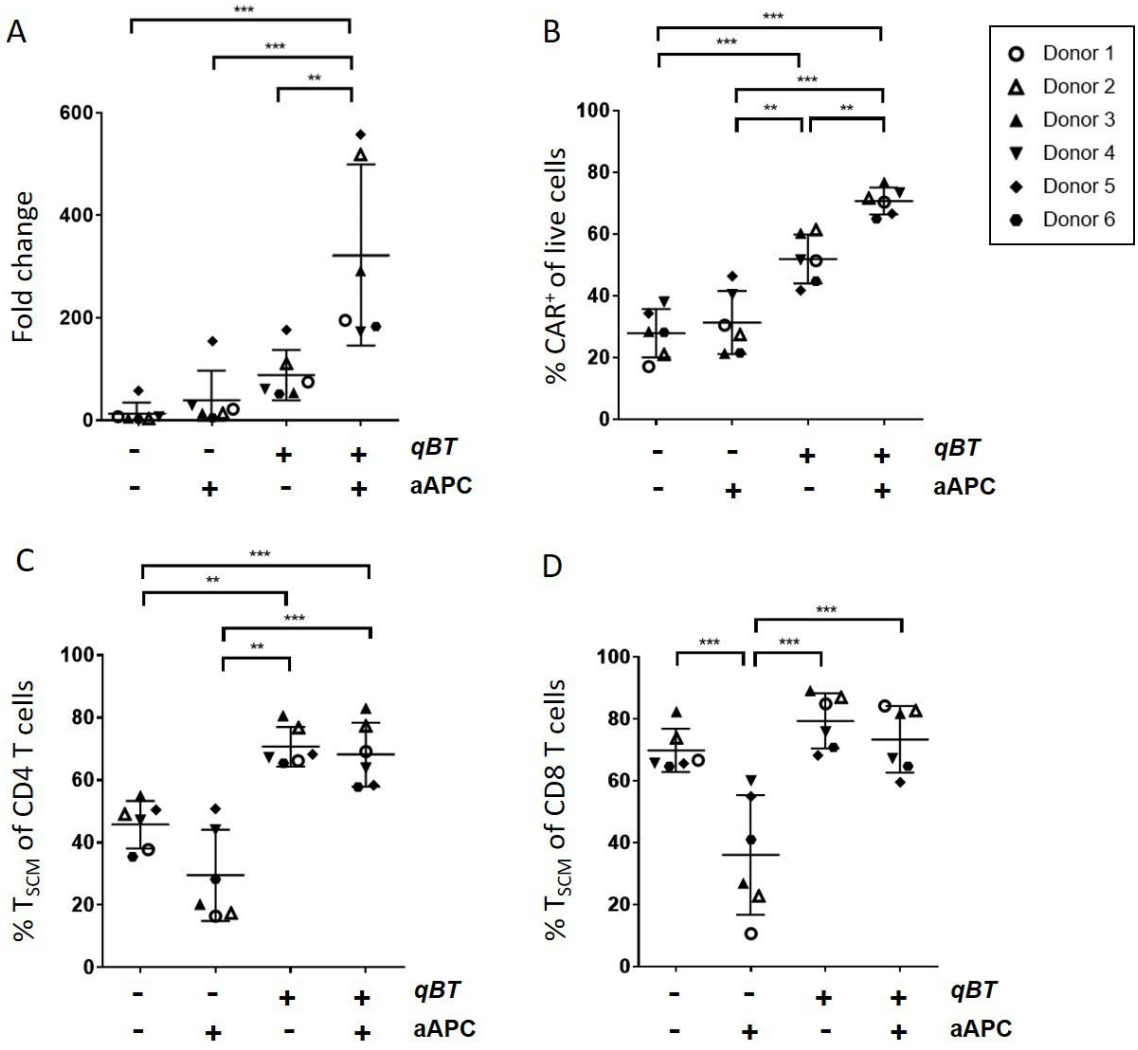

Figure 5. The effect of different *iCellar*™ combinations on characteristics of CAR-T cells produced by *qCART*™

Human peripheral blood mononuclear cells (PBMC) electroporated with *Quantum pBac*™ expressing CAR and cultured for 10 days in the presence or absence of aAPC and/or *Quantum Booster*™ (*qBT*) were harvested and assessed for (A) cell expansion fold change, (B) percentage of CAR^+ cells, and percentage of T_{SCM} cell subsets in (C) $CD4^+$ or (D) $CD8^+$ cells. Data shown are from six healthy donors. Horizontal lines represent the mean and s.e.m. fold change (A), mean and s.e.m. percentage of CAR^+ cells (B), and mean and s.e.m. percentage of T_{SCM} cell subsets (C and D). * $p < 0.05$, ** $p < 0.01$, *** $p < 0.001$.

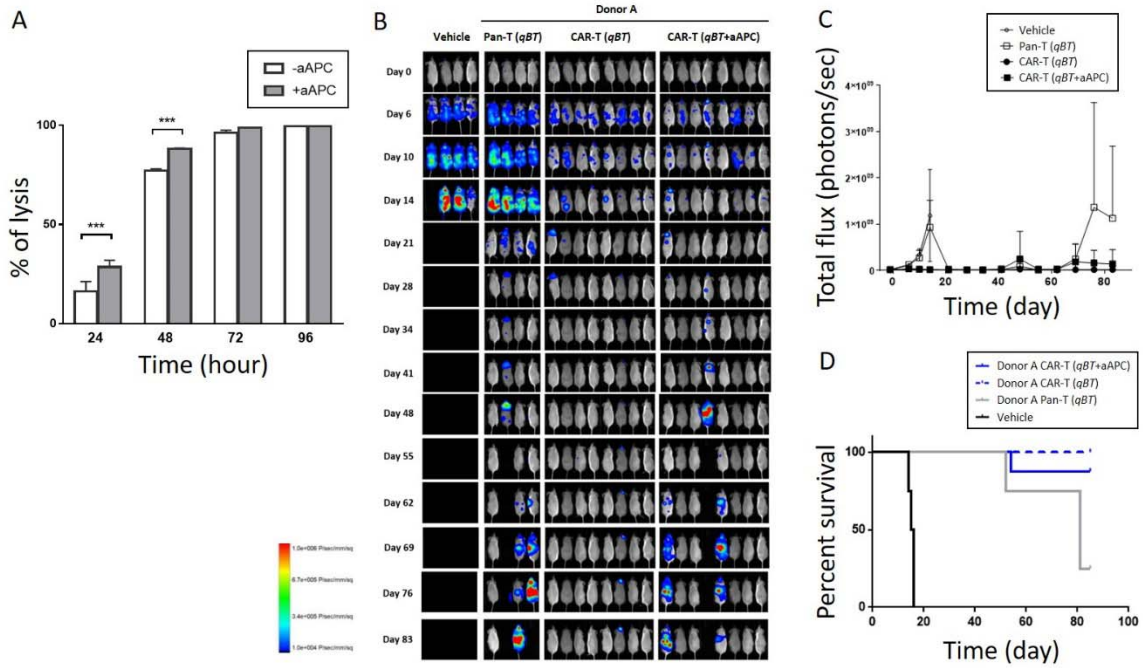

Figure 6. *In vitro* and *in vivo* functional characterization of CAR-T cells produced using the *qCART*™ system

(A) *In vitro* cytotoxicity of CAR-T cells (E:T ratio of 1:1) with or without pre-incubation with aAPC, on Raji-GFP/Luc target cells. (B) *In vivo* cytotoxicity of CAR-T cells with or without pre-incubation with aAPC in Raji-GFP/Luc-bearing immunodeficient mice. Fluorescence intensity values (C) and survival curves (D) of mice from (B) plotted against time. Results shown are from four to eight mice/group. T cells were obtained from a representative donor. Vehicle and Pan-T cells were used as controls. *Quantum Booster*™ (*qBT*) was present in all cell culture conditions. *** $p < 0.001$.

Table 1. Finding optimal BCMA CAR-T cells

Human peripheral blood mononuclear cells (PBMC) electroporated with *Quantum pBac*™ expressing anti-BCMA CARs were analyzed for their performance, including cell expansion (Day 1 to 10 fold change), percentage of CAR^+ cells, CD8/CD4 ratio, percentage of T_{SCM} cell subsets in $CD4^+$ or $CD8^+$ cells, and cytotoxicity against $BCMA^+$ cells. Data shown are from four healthy donors.

Group	N (independent experiments)	Day 1 to 10 fold change	% CAR^+	CD8/CD4 ratio	% T_{SCM} in $CD4^+$	% T_{SCM} in $CD8^+$	% $PD1^+$ in CAR^+	Cytotoxicity against $BCMA^+$ cells (5:1, 48hr)
aBCMA-1	2	168 (101, 236)	45.8 (45.0, 46.6)	1.3 (0.9, 1.7)	60.3 (59.5, 61.1)	74.6 (73.3, 75.9)	NA	15.8 (14.7, 16.8)
aBCMA-2	7	226 (141~384)	63.7 (55.3~74.5)	1.5 (0.4~3.8)	71.0 (63.3~80.6)	76.3 (63.3~83.1)	0.8 (0.6~1.7)	55.3 (46.0~71.5)
aBCMA-3	3	289 (162~472)	51.6 (33.9~73.4)	2.7 (1.4~4.2)	76.6 (67.6~84.7)	82.4 (754~87.4)	74.6 (49.9~90.4)	9.8 (3.3~14.2)
aBCMA-4	2	223 (149, 297)	57.8 (50.5, 65.1)	3.4 (1.8, 5)	68.1 (64.9, 71.3)	69.5 (57.4, 81.6)	6.4 (1.2, 11.5)	12.5 (11.7, 13.2)
aBCMA-5	3	278 (187~454)	68.3 (68.1~68.5)	2.5 (1.9~3.7)	73.6 (67.1~80.4)	79.7 (71.7~85.7)	0.6 (0.4~ 1.1)	50.5 (43.2~57.5)

Table 2. Evaluation of different transgene sizes on CAR-T cell performance

Donor T cells were electroporated with *Quantum pBac*™ expressing transgenes with sizes ranging from 3.0 kb to 7.6 kb. The percentages of CAR^+ T cells, expansion fold and relative distribution of T_{SCM} cell subsets in $CD4^+$ CAR+ and $CD8^+$ CAR^+ T cell subtypes are shown. Data shown are from two to 11 healthy donors.

	Multiple Myeloma (MM)		Hematopoietic B Cell Malignancy			
Transgene (size)	Target X (3.0 kb)	Target Y (3.0 kb)	CD20/CD19 (3.7 kb)	CD20/CD19 + iCas9 (5.2 kb)	CD20/CD19 + modulator A (5.4 kb)	CD20/CD19 + modulator B (7.6 kb)
Number of donors tested	2	2	11	10	3	3
% CAR^+	77.3 ~ 83.9	80.6 ~ 88.3	54.4 ~ 79.0	44.3 ~ 67.8	42.0 ~ 47.7	28.7 ~ 42.7
Expansion fold	1,507 ~ 1,910	1,790 ~ 4,190	103 ~ 1,501	406 ~ 2,090	85 ~ 315	75 ~ 190
% T_{SCM} in $CD4^+$: In $CD8^+$:	68.0 ~ 86.8 67.2 ~ 77.2	74.3 ~ 82.4 76.5 ~ 76.5	18.2 ~ 65.8 45.8 ~ 83.4	65.1 ~ 92.7 66.7 ~ 92.9	46.2 ~ 61.9 57.9 ~ 70.6	N.D. 62.5 ~ 74.1